SCIENCE CHINA
Chemistry

• ARTICLES •
• SPECIAL TOPIC • Frontiers in Polymer Science

December 2016 Vol.59 No.12: 1593–1599
doi: 10.1007/s11426-016-0247-9

Self-host yellow iridium dendrimers based on carbazole dendrons: synthesis, characterization and application in solution-processed organic light-emitting diodes

Bin Wang, Shiyang Shao, Junqiao Ding*, Lixiang Wang*, Xiabin Jing & Fosong Wang

State Key Laboratory of Polymer Physics and Chemistry, Changchun Institute of Applied Chemistry, Chinese Academy of Sciences, Changchun 130022, China

Received May 30, 2016; accepted June 29, 2016; published online October 25, 2016

On the basis of different generation carbazole dendrons, a series of self-host yellow Ir dendrimers (**Y-G0**, **Y-G1** and **Y-G2**) have been successfully synthesized and characterized in detail. It is found that the peripheral dendrons can effectively reduce the intermolecular interactions between emissive Ir cores, as verified by the increased photoluminescence quantum yields and film lifetimes. Among these dendrimers, **Y-G2** bearing the second generation dendrons shows the best non-doped device performance, revealing a peak luminous efficiency of 20.2 cd/A. The value is nearly twice that of **Y-G0** without any dendrons, which could be further improved to 32.1 cd/A by dispersing **Y-G2** into a host matrix. We believe that this work will shed light on the development of highly efficient yellow phosphorescent dendrimers with a self-host strategy.

iridium, dendrimers, carbazole, self-host, solution-processed OLEDs

Citation: Wang B, Shao S, Ding J, Wang L, Jing X, Wang F. Self-host yellow iridium dendrimers based on carbazole dendrons: synthesis, characterization and application in solution-processed organic light-emitting diodes. *Sci China Chem*, 2016, 59: 1593−1599, doi: 10.1007/s11426-016-0247-9

1 Introduction

Solution-processed organic light-emitting diodes (OLEDs) are highly desirable for low-cost, large-area next-generation display and lighting technologies [1–7]. Among the many different kinds of available emitting materials, dendrimers show the greatest potential since they possess the advantages of not only well-defined structures of small molecules but also film-forming processibility of polymers [8,9]. In particular, phosphorescent iridium (Ir) dendrimers exhibit promising device performance because they allow both singlet and triplet excitons to generate unique emission with a theoretical internal quantum efficiency of 100%.

Generally, Ir dendrimers consist of an emissive Ir complex core, peripheral dendrons and surface groups. Up to now, the used dendrons for Ir dendrimers have fallen into two categories: those that are electrically insulating and merely play a structural role in controlling the intermolecular interactions (e.g. Fréchet dendrons [10] and Müllen dendrons [11]), and those that are electroactive and play additional roles in carrier transporting (e.g. carbazole dendrons [12–18] and arylamine dendrons [19,20]). The latter case makes it possible to fabricate efficient solution-processed OLEDs with a non-doped device configuration, avoiding the need of a host. For this purpose, our group [12,13,16] have demonstrated a series of self-host blue, green and red Ir dendrimers based on carbazole dendrons, where the dendritic wedge can act as the host of the central core by itself. As a result, non-doped devices with external quantum efficiencies (EQEs) higher than 10% are realized. However, yellow Ir dendrimers with a self-host feature are rarely re-

*Corresponding authors (email: junqiaod@ciac.ac.cn; lixiang@ciac.ac.cn)

ported even though they are indispensable not only to generate white electroluminescence (EL) when mixed with sky-blue dyes, but also to improve the power efficiency of white OLEDs [21,22].

In this paper, we develop a series of self-host yellow Ir dendrimers bearing 0–2 generation carbazole dendrons (**Y-G0**, **Y-G1** and **Y-G2**), and research their photophysical, electrochemical and EL properties in detail. With the increasing generation number, it is found that the intermolecular interactions and thereby luminescence quenching can be effectively prohibited. Correspondingly, the non-doped device efficiency is gradually enhanced from 10.2 cd/A of **Y-G0** to 14.1 cd/A of **Y-G1** and 20.2 cd/A of **Y-G2**. Given the obtained best non-doped device performance, the dendrimer **Y-G2** is further dispersed into a host matrix to fabricate doped devices, revealing an improved luminous efficiency as high as 32.1 cd/A together with Commission Internationale de L'Eclairage (CIE) coordinates of (0.52, 0.48).

2 Experimental

2.1 Materials

Chemicals and reagents including *N*-(4-phenyl)-*o*-phenylenediamine, $Ir(acac)_3$, *n*-BuLi, *N*,*N*-dimethylformamide (DMF), 18-crown-6, $AgSO_3CF_3$, mesitylene, $Pd(OAc)_2$, $H^tBu_3P{\cdot}BF_4$, 18-crown-6, CuI, K_2CO_3 and *t*-BuONa were used as purchased from Acros Organics (USA) without further purification. Solvents for chemical synthesis were purified according to the standard procedures. 9,9′-Dioctyl-2-bromofluorene, the first and second generation carbazole dendrons (**D1** and **D2**) were fabricated by our lab.

2.2 Experimental information

2.2.1 9,9-Dioctyl-9*H*-fluorenyl-2-formaldehyde (**1**)

Under argon, *n*-BuLi (2.50 M, 2.92 mL) was added dropwise to a solution of 9,9′-dioctyl-2-bromofluorene (2.00 g, 6.64 mmol) in 50 mL tetrahydrofuran at −78 °C. After the mixture was aged for 30 min, dry *N*,*N*-dimethylformamide (1.03 mL, 13.30 mmol) was added slowly, and then the reaction solution was allowed to return to ambient temperature. After stirring for 12 h, 50 mL of water was added to quench the reaction. The mixture was extracted with dichloromethane (3×30 mL). The combined organic phases were washed with brine, dried over Na_2SO_4 and then concentrated under reduced pressure to give a crude compound. The crude product was purified by column chromatography on silica gel using petroleum ether/dichloromethane (2:1) as eluent to give the product (1.58 g) in 95% yield. ^{1}H NMR (400 MHz, $CDCl_3$): δ 10.05 (s, 1H), 8.13–8.06 (m, 1H), 7.87–7.83 (m, 2H), 7.80–7.77 (m, 1H), 7.42–7.36 (m, 3H), 2.05–1.94 (m, 4H), 1.20–1.17 (m, 4H), 1.10–1.03 (m, 16H), 0.83–0.80 (m, 6H), 0.60–0.55 (m, 4H).

2.2.2 1-Phenyl-2-(9,9-dioctyl-9*H*-fluoren-2-yl)-1*H*-benzoimidazole (**LG0**)

A mixture of *N*-(4-phenyl)-*o*-phenylenediamine (1.80 g, 10.00 mmol), 9,9-dioctyl-9*H*-fluorene-2-carbaldehyde (4.20 g, 10.00 mmol) were dissolved in the mixed solvent of 30 mL ethoxyethanol and 5 mL ethanol. The reaction system was heated at 160 °C for 48 h under argon. After cooling to room temperature (r.t.), the mixture was quenched by H_2O (50 mL), extracted with EtOAc (4×20 mL), and the combined extracts were dried over anhydrous Na_2SO_4. After the solvent had been completely removed, the residuewas purified by column chromatography on silica gel with petroleum/EtOAc (10:1) as the eluent to give the product in a yield of 35% (1.90 g).^{1}H NMR (300 MHz, $CDCl_3$, δ): 7.92 (d, *J*=7.8 Hz, 1H), 7.78 (d, *J*=7.2 Hz, 1H), 7.69 (m, 2H), 7.52–7.45 (m, 3H), 7.37–7.27 (m, 9H), 1.83 (m, 2H), 1.65 (m, 2H), 1.25–1.08 (m, 12H), 0.96 (s, 8H), 0.89 (t, *J*=7.2 Hz, 6H), 0.42 (br, 4H).

2.2.3 1-(4-Bromophenyl)-2-(9,9-dioctyl-9*H*-fluoren-2-yl)-1*H*-benzoimidazole (**2**)

N-(4-bromophenyl)-*o*-phenylenediamine (6.00 g, 22.80 mmol) and 9,9-dioctyl-9*H*-fluorene-2-carbaldehyde (9.00 g, 22.80 mmol) were added to ethoxyethanol (30 mL). Then, 30% H_2O_2 (159.60 mmol) and 37% HCl (79.80 mmol) were added and the mixture was stirred at r.t. for 24 h. The reaction was quenched by H_2O (50 mL), extracted with EtOAc (4×20 mL), and the combined extracts were dried over anhydrous Na_2SO_4. After removing the solvent completely, the residue was purified by column chromatography on silica gel with petroleum/EtOAc (10:1) as the eluent to give the product in a yield of 55% (7.80 g). ^{1}H NMR (300 MHz, $CDCl_3$, δ): 7.92 (d, *J*=7.8 Hz, 1H), 7.73 (m, 3H), 7.62 (m, 2H), 7.39–7.2 (m, 9H), 1.86 (m, 2H), 1.68 (m, 2H), 0.92–1.22 (m, 20H), 0.80 (t, *J*=6.7 Hz, 6H), 0.46 (m, 4H).

2.2.4 Ligand **LG1**

A mixture of **2** (1.30 g, 2.00 mmol), **D1** (0.80 g, 3.00 mmol), CuI (48 mg, 0.25 mmol), 18-crown-6 (50 mg, 0.20 mmol), K_2CO_3 (0.60 g, 4.50 mmol) and 1,3-dimethyl-3,4,5,6-tetrahydro-2(1*H*)-pyrimidinone (DMPU) (2 mL) was heated at 190 °C for 24 h under argon. After cooling to room temperature, the reaction was quenched with 1 N hydrochloric acid. The mixture was extracted with dichloromethane (CH_2Cl_2) (4×30 mL), and the combined organic phases were washed with $NH_3{\cdot}H_2O$ and water sequentially, dried over Na_2SO_4, and then filtered. After the solvent had been removed, the residue was purified by column chromatography on silica gel with petroleum/CH_2Cl_2 (10:1) as eluent to give **LG1** with a yield of 59% (1.00 g). ^{1}H NMR (300 MHz, $CDCl_3$, δ): 8.16 (d, *J*=1.4 Hz, 2H), 7.95–7.98 (m, 1H), 7.72 (m, 5H), 7.29–7.58 (m, 16H), 1.84 (m, 4H), 1.47 (m, 18H), 1.05 (m, 4H), 0.92 (m, 4H), 0.89 (br, 12H), 0.72 (t, *J*=7.0 Hz, 6H), 0.49 (br, 4H).

2.2.5 Ligand **LG2**

This compound was prepared the same as the procedure for the synthesis of **LG1** in a yield of 55% (1.60 g). ^{1}H NMR (300 MHz, $CDCl_3$, δ): 8.26 (d, *J*=1.6 Hz, 2H), 8.17 (d, *J*=1.6 Hz, 4H), 8.00 (d, *J*=8.3 Hz, 1H), 7.92 (d, *J*=8.5 Hz, 2H), 7.86 (d, *J*=7.4 Hz, 1H), 7.77 (d, *J*=4.0 Hz, 1H), 7.74 (t, *J*=4.8 Hz, 3H), 7.72 (d, *J*=8.6 Hz, 2H), 7.68 (dd, *J*=8.6, 1.7 Hz, 2H), 7.52 (s, 1H), 7.47 (dd, *J*=8.6, 1.8 Hz, 5H), 7.41 (t, *J*=8.6 Hz, 2H), 7.35 (s, 2H), 7.32 (t, *J*=4.6 Hz, 5H), 1.87 (m, 4H), 1.47 (s, 36H), 1.06 (m, 4H), 0.96 (m, 4H), 0.87 (s, 12H), 0.71 (t, *J*=7.4 Hz, 6H), 0.50 (m, 4H).

2.2.6 Dendrimer **Y-G0**

A mixture of **LG0** (1.55 g, 2.66 mmol), $Ir(acac)_3$ (0.44 mg, 0.89 mmol) and glycerol (50 mL) were refluxed under argon for 24 h. After cooling to r.t., the mixture was poured into water and then extracted with CH_2Cl_2. The organic extracts were washed with water and dried over anhydrous sodium sulfate. After the solvent had been completely removed, the residue was purified by column chromatography on silica gel with petroleum/CH_2Cl_2 (5:1) as the eluent to afford **Y-G0** in a yield of 37% (0.65 g). ^{1}H NMR (300 MHz, $CDCl_3$, δ): 7.73 (s, 12H), 7.58 (d, *J*=7.2 Hz, 3H), 7.69 (m, 3H), 7.31–7.17 (m, 15H), 7.09 (t, *J*=7.2 Hz, 3H), 6.99 (t, *J*=7.2 Hz, 3H), 6.69 (s, 3H), 6.62 (d, *J*=8.0 Hz, 3H), 1.87–1.48 (m, 12H), 1.31 (br, 48H), 1.05 (br, 12H), 0.97 (t, *J*=7.2 Hz, 18H), 0.69 (br, 12H). MALDI-TOF (matrix assisted laser desorption ionization/time-of-flight) (*m*/*z*): Calcd. For $C_{126}H_{147}N_6Ir$: 1937.13; found: 1937.10. Anal. calcd. for $C_{126}H_{147}N_6Ir$: C, 78.10%; H, 7.65%; N, 4.34%; found: C, 78.15%; H, 7.81%; N, 4.30%.

2.2.7 Dendrimer **Y-G1**

LG1 (1.25 g, 1.45 mmol) and $Ir(acac)_3$ (0.24 mg, 0.48 mmol) were added to the mixed solvent of glycerol (30 mL) and tetraethylene glycol (5 mL), then the reaction was refluxed under argon for 24 h. After cooling to r.t., the mixture was poured into water and extracted with CH_2Cl_2. The organic extracts were washed with water and dried over anhydrous sodium sulfate. After the solvent being completely removed, the residue was purified by column chromatography on silica gel with petroleum/CH_2Cl_2 (4:1) as the eluent to afford **Y-G1** in a yield of 25% (0.20 g).^{1}H NMR (300 MHz, $CDCl_3$, δ): 8.20 (s, 6H), 7.92–7.80 (m, 12H), 7.55 (s, 15H), 7.37 (d, *J*=7.2 Hz, 3H), 7.18 (d, *J*=7.2 Hz, 3H), 7.12 (d, *J*=7.2 Hz, 3H), 7.00–6.90 (m, 12H), 6.62 (br, 3H), 5.99 (br, 3H), 2.00–1.50 (m, 12H), 1.51 (s, 54H), 1.01 (m, 48H), 0.95–0.75 (m, 12H), 0.72 (t, *J*=7.0 Hz, 18H), 0.63 (br, 12H). MALDI-TOF (*m*/*z*): Calcd. For $C_{186}H_{216}N_9Ir$: 2769.98; found: 2769.75. Anal. calcd. for $C_{186}H_{216}N_9Ir$: C, 80.65%; H, 7.86%; N, 4.55%; found: C, 80.77%; H, 7.81%; N, 4.59%.

2.2.8 Intermediate complex **3**

$IrCl_3{\cdot}3H_2O$ (0.35 g, 1.00 mmol) and the brominated ligand **2** (1.32 g, 2.00 mmol) were added to the mixed solvent of ethoxyethanol/H_2O (30 mL:10 mL). The mixture was kept at reflux for 24 h. After cooling to r.t., the precipitate was collected by filtration, and washed with water and ethanol sequentially. Then the obtained chloro-bridged iridium dimer was fully dried and used for next step reaction directly. The intermediate dimer, **2** (0.90 g, 1.32 mmol), $AgSO_3CF_3$ (0.31 g, 1.20 mmol) and K_2CO_3 (0.42 g, 3.00 mmol) were added to mesitylene (50 mL) under argon, and the reaction was refluxed for 10 h. After cooling to r.t., the solvent was removed at 50 °C under reduce pressure. The residue was purified by column chromatography on silica gel with petroleum/CH_2Cl_2 (8:1) as the eluent to afford **3** in a yield of 50% (1.30 g). ^{1}H NMR (300 MHz, $CDCl_3$, δ): 7.69 (t, *J*=6.9 Hz, 6H), 7.45 (d, *J*=8.4 Hz, 3H), 7.35–7.26 (m, 6H), 7.17–7.02 (m, 18H), 6.96 (t, *J*=7.2 Hz, 3H), 6.86–6.81 (m, 3H), 6.42 (d, *J*=7.8 Hz, 3H), 1.79–1.39 (m, 12H), 1.23–0.99 (m, 48H), 0.93 (br, 12H), 0.81 (t, *J*=6.6 Hz, 18H), 0.53 (br, 12H).

2.2.9 Dendrimer **Y-G2**

A mixture of **3** (1.30 g, 0.60 mmol), **D2** (1.95 g, 2.70 mmol), $Pd(OAc)_2$ (12 mg), $H^tBu_3P{\cdot}BF_4$ (94 mg) and *t*-BuONa (0.26 g, 2.70 mmol) was degassed for 30 min, then mesitylene (100 mL) was added under argon. The reaction was kept at reflux for 48 h. The mixture was cooled to r.t., and then the solvent was removed at 50 °C under reduce pressure. The crude product was purified by column chromatography on silica gel with petroleum/CH_2Cl_2 (5:1) as the eluent to afford **Y-G2** in a yield of 49% (1.20 g). ^{1}H NMR (300 MHz, $CDCl_3$, δ): 8.31 (s, 6H), 8.18 (s, 12H), 8.02 (s, 9H),7.88 (d, *J*=9.0 Hz, 3H), 7.82 (d, *J*=8.6 Hz, 6H), 7.72 (dd, *J*=8.6, 1.5 Hz, 6H), 7.48 (dd, *J*=8.6, 1.6 Hz, 12H), 7.38 (d, *J*=8.8 Hz, 18H), 7.18 (t, *J*=8.4 Hz, 9H), 7.11–6.93 (m, 15H), 2.00–1.60 (m, 12H), 1.48 (s, 108H), 1.14–0.97 (m, 48H), 0.97–0.78 (m, 12H), 0.67 (t, *J*=7.0 Hz, 18H), 0.61 (br, 12H). MALDI-TOF (*m*/*z*): Calcd. For $C_{282}H_{306}N_{15}Ir$: 4097.76; found: 4097.67. Anal. calcd. for $C_{282}H_{306}N_{15}Ir$: C, 82.66%; H, 7.53%; N, 5.13%; found: C, 82.62%; H, 7.59%; N, 5.08%.

2.2.10 Measurement and characterization

^{1}H NMR spectra were recorded with Bruke Avance 300 NMR spectrometer (Germany). The elemental analysis was performed using a Bio-Rad elemental analysis system. MALDI-TOF mass spectra were performed on AXIMA CFR MS apparatus (Shimadzu, Japan). Cyclic voltammetry experiments were performed on an EG&G 283 (Princeton Applied Research, USA) potentiostat/galvanostat system. All measurements were carried out with a conventional three-electrode system consisting of a platinum working electrode, a platinum counter electrode and an Ag/AgCl reference electrode. The supporting electrolyte was 0.1 M tetrabutylammonium perchlorate(*n*-Bu_4NClO_4). The ferrocene was used as a standard to calibrate the system. The

UV-Vis absorption and photoluminescence spectra were measured by Perkin-Elmer Lambda 35 UV-Vis spectrometer (USA) and Perkin-Elmer LS 50B spectrofluorometer (USA), respectively. Solution spectra were recorded in CH_2Cl_2 or toluene with a concentration of 10^{-5} M. Thin films onto quartz for spectroscopic measurements were prepared by spin-coating. All the above experiments and measurements were carried out at room temperature under ambient conditions. Solution photoluminescent (PL) quantum efficiency was measured in degassed toluene solution using freeze-pump-thaw procedure and *fac*-Ir(ppy)$_3$ (Φ_{pl}= 0.40 in toluene) was used as the reference. Phosphorescence spectra at 77 K were measured in a toluene-ethanol-methanol (5:4:1) mixed solvent. The triplet energies were estimated as the maximum of the first vibronic mode ($S_0^{\nu=0} \leftarrow T_1^{\nu=0}$) of the corresponding phosphorescence spectra at 77 K. The PL decay curves were obtained from a Lecroy Wave Runner 6100 digital oscilloscope (1 GHz) by using a tunable laser (pulse width=4 ns, gate=50 ns) as excitation source (Continuum Sunlite OPO) and the lifetimes of phosphorescence from the samples were measured in solid films at 298 K under the argon.

2.2.11 Device fabrication and measurement

The indium-tin oxide (ITO) glass plates were cleaned in ultrasonic solvent bath and then baked in a heating chamber at 120 °C, and treated with O_2 plasma for 25 min before use. A 50 nm thick ITO-modifying layer of poly(3,4-ethylenedioxythiophene):poly(styrenesulfonate) (PEDOT:PSS) was spin-coated on top of ITO and then baked for 40 min at 120 °C. The emitting layer was then prepared by spin-coating from the chlorobenzene solution of the dendrimer at the concentration of 10 mg/mL. After that, the substrate was transferred to a vacuum thermal evaporator. Successively, 60 nm thick TPBI was deposited, followed by the deposition of LiF/Al (1 nm:100 nm) at a base pressure of less than 10^{-6} Torr (1 Torr=133.32 Pa). The active emissive area was 10 mm^2. EL spectra, CIE coordinates, current-voltage and brightness-voltage characteristics of devices were measured with a Spectra scan PR650 spectrophotometer (Photo Research Inc., USA) at the forward direction and a computer-controlled Keithley 2400 (USA) under ambient condition.

3 Results and discussion

3.1 Synthesis

The synthetic route of the yellow Ir dendrimers is shown in Scheme 1. At first, the ligand **LG0** and the key intermediate

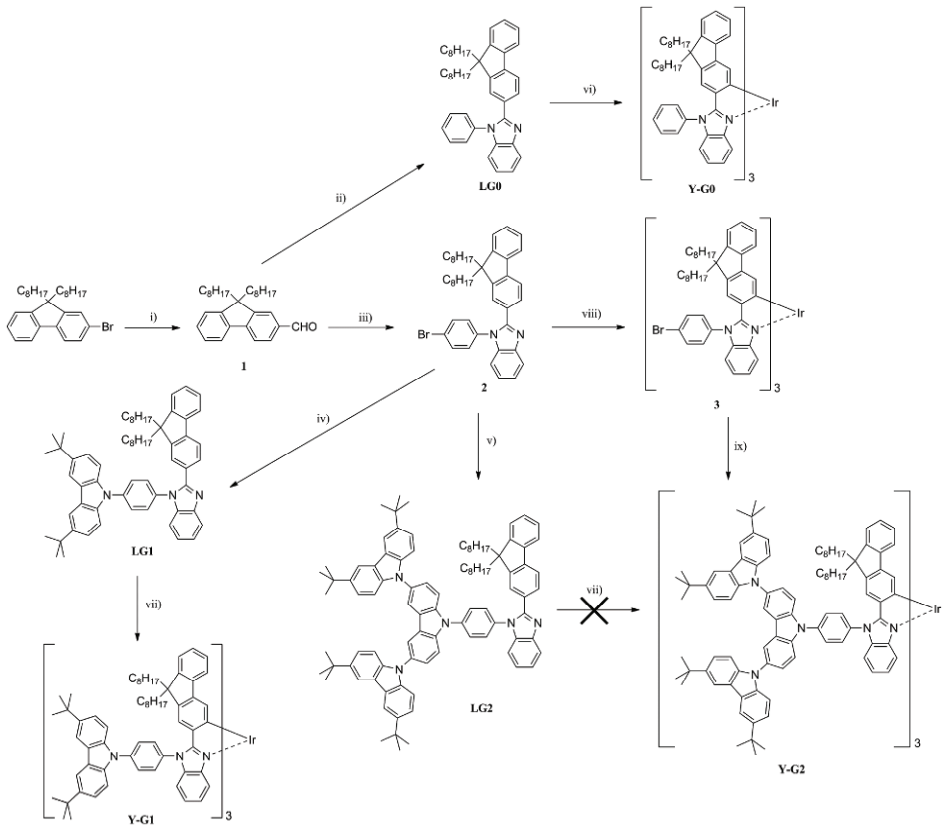

Scheme 1 Synthetic routes of the yellow-emitting Ir dendrimers. Conditions: i) (a) *n*-BuLi, tetrahydrofuran (THF), −78 °C, (b) *N*,*N*-dimethylformamide (DMF), −78 °C; ii) *N*-(4-phenyl)-*o*-phenylenediamine, ethoxyethanol/EtOH, reflux, 48 h; iii) *N*-(4-bromophenyl)-*o*-phenylenediamine, H_2O_2/HCl, ethoxyethanol, r.t. 24 h; iv) **D1**, CuI, K_2CO_3, 18-crown-6, DMPU, 190 °C, 24 h; v) **D2**, CuI, K_2CO_3, 18-crown-6, DMPU, 190 °C, 24 h; vi) Ir(acac)$_3$, glycerol, 200 °C, 24 h; vii) Ir(acac)$_3$, tetraethylene glycol, 230 °C, 24 h; viii) (a) $IrCl_3 \cdot 3H_2O$, ethoxyethanol/H_2O=3:1 (*v*/*v*), reflux, 24 h, (b) **3**, $AgSO_3CF_3$, K_2CO_3, mesitylene, reflux, 10 h; ix) **D2**, Pd(OAc)$_2$, H^{t}Bu$_3$P·BF$_4$, *t*-BuONa, mesitylene, reflux, 48 h.

1-(4-bromophenyl)-2-(9,9-dioctyl-9*H*-fluoren-2-yl)-1*H*-benzoimidazole (**2**) were prepared by the cyclization between 9,9-dioctyl-fluorene-2-carbaldehyde (**1**) and *N*-phenylbenzene-1,2-diamine or *N*-(4-bromophenyl)benzene-1,2-diamine. Subsequently, **2** was coupled with the first and second-generation carbazole dendrons (**D1** and **D2**) via a Ullmann reaction to afford the dendritic ligand **LG1** and **LG2**, respectively. The corresponding Ir dendrimers were finally synthesized by the coordination between the ligands and $Ir(acac)_3$ in high-boiling-point solvents, such as glycerol and tetraethylene glycol. An acceptable moderate yield of 25%–37% was obtained for **Y-G0** and **Y-G1**. Unfortunately, the yield of **Y-G2** was extremely lower than 5%, attributable to the poor solubility in such solvents. To solve this problem, a post-dendronization strategy was performed. The bromide-functionalized Ir core (**3**) was firstly synthesized, and then reacted with the second-generation dendron to produce the resultant dendrimer **Y-G2** with an improved yield of 25%. The molecular structures of **Y-G0–Y-G2** were verified by ^{1}H NMR spectroscopy, elemental analysis, and MALDI-TOF mass spectrometry. And all the dendrimers are well soluble in common organic solvents, such as dichloromethane (CH_2Cl_2), chloroform, chlorobenzene and toluene at r.t..

3.2 Photophysical and electrochemical properties

Figure 1 shows the absorption spectra of **Y-G0**, **Y-G1** and **Y-G2** in CH_2Cl_2 as well as the PL spectra in film states. As one can see, the intense absorption bands below 360 nm are assigned to the spin-allowed ligand-centered (LC) transitions, while the weak absorptions in the range of 360–550 nm are ascribed to the metal-to-ligand charge-transfer (MLCT) transitions. Moreover, the characteristic absorption located at about 246 nm, corresponding to the carbazole unit, becomes much stronger with the increasing dendron generation. Estimated from the onset of the absorption spectra, nearly the same optical band gap (2.20–2.21 eV) is observed for all Ir dendrimers. This suggests that the introduction of the carbazole dendrons does not greatly affect the optical property of the Ir core.

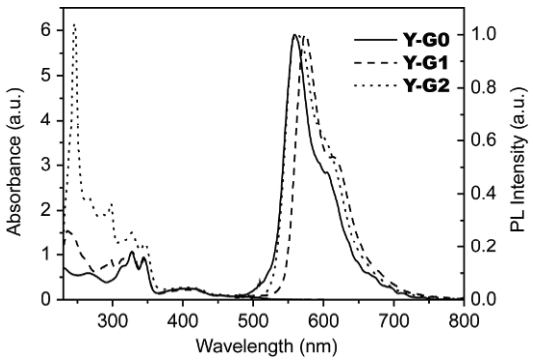

Figure 1 Absorption spectra of the Ir dendrimers in CH_2Cl_2 at a concentration of 10^{-5} M and PL spectra in film state.

As depicted in Figure 1, the film emission peak is initially red-shifted from 559 nm of **Y-G0** to 574 nm of **Y-G1**, mainly induced by the enlarged conjugation length. With the incorporation of even higher generation dendrons, **Y-G2** shows a blue-shifted PL spectrum relative to **Y-G1**, indicative of the reduced intermolecular interactions. On going from **Y-G0** to **Y-G1** and **Y-G2**, the solution PL quantum yield is up from 0.45 to 0.70 and 0.85. Meanwhile, although **Y-G0–Y-G2** all show similar PL decay behaviors in toluene solution, the film lifetime of **Y-G2** is found to be much longer than those of **Y-G1** and **Y-G0** (Table 1). These observations are in well agreement with the proposal that the intermolecular interactions of the Ir cores can be inhibited by the large carbazole dendrons.

The electrochemical behaviors of the dendrimers were investigated by cyclic voltammetry (CV) method. The highest occupied molecular orbital (HOMO) energy levels were determined from the onset of the oxidation potentials, and the lowest unoccupied molecular orbital (LUMO) energy levels were deduced according to the HOMO levels together with the optical band gap (E_g). It should be noted that, all the dendrimers have close HOMO levels of −4.78– −4.84 eV and LUMO levels of −2.57– −2.68 eV. That is to say, the electrochemical properties are almost independent on the outer dendrons, consistent with the above-mentioned optical counterparts.

3.3 Electroluminescent performance

To explore the EL performance of these Ir dendrimers, solution-processed OLEDs with a non-doped configuration of indium tin oxide (ITO)/poly(3,4-ethylenedioxythiophene): poly(styrene sulfonic acid) (PEDOT:PSS)/EML/1,3,5-tris(2-*N*-phenylbenzimidazolyl)benzene (TPBI)/LiF/Al were firstly fabricated (Figure 2). Herein the dendrimers alone were used as the neat emitting layer (EML), and TPBI acted as the electron transporting/hole blocking layer. As can be clearly seen in Figure 3(a), the EL spectra, independent on the driving voltage from 5 to 12 V, are similar to the PL ones with the main peak located at 564–568 nm accompanied by a shoulder at around 610 nm. The CIE coordinates are (0.51, 0.49), (0.52, 0.48) and (0.53, 0.47) for **Y-G0**, **Y-G1** and **Y-G2**, respectively. Furthermore, no emission from the carbazole dendrons or TPBI is observed, indicating

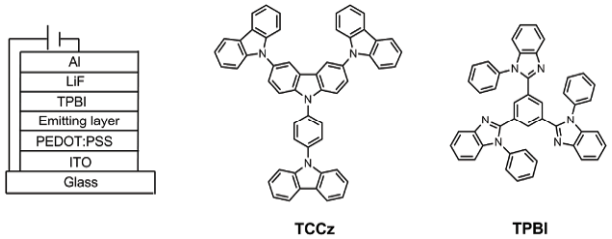

Figure 2 Schematic diagram of the device configurations, and chemical structures of the host material as well as the hole-blocking material.

Table 1 Photophysical properties of the Ir dendrimers

	λ_{abs} (logε) (nm) [a]	λ_{em} (nm) [b]	λ_{em} (nm) [c]	Φ [d]	τ (μs) [e]	τ_1 (μs) [f]	A_1 [g]	τ_2 (μs) [f]	A_2 [g]	E_g (eV) [h]	E^{ox} (V) [i]	HOMO (eV)	LUMO (eV)
Y-G0	266 (4.8), 344 (4.9), 404 (4.4), 452 (4.0), 488 (3.8), 541 (3.0)	555	559	0.45	1.49	0.02	0.07	0.11	0.93	2.21	–0.02	4.78	2.57
Y-G1	236 (5.2), 328 (5.0), 345 (4.9), 403 (4.4), 452 (4.0), 488 (3.8), 541 (3.0)	557	574	0.70	1.62	0.03	0.14	0.12	0.86	2.21	0.04	4.84	2.63
Y-G2	266 (5.4), 298 (5.3), 404 (4.4), 453 (4.0), 489 (3.8), 542 (3.0)	557	562	0.85	1.55	0.05	0.24	0.26	0.76	2.20	0.08	4.88	2.68

a) Measured in CH_2Cl_2 at 298 K at a concentration of 10^{-5} M. b) Measured in toluene at 298 K at a concentration of 10^{-5} M. c) Measured in neat flim at 298 K and the excitation wavelength was 410 nm. d) PL quantum efficiency measured in degassed toluene solution using freeze-pump-thaw procedure for all the dendrimers. The excitation wavelength was 410 nm, and *fac*-Ir(ppy)$_3$ was used as the reference for the quantum yield measurement. (e) Lifetimes measured in toluene by using monoexponential fit of emission decay curves. (f) Lifetimes measured in solid films in the argon and the data are obtained by biexponential fit of emission decay curves. (g) The relative percentage of the biexponential fit of solid state emission. (h) Estimated from the onset of the absorption spectra. (i) Onset of the oxidation potential.

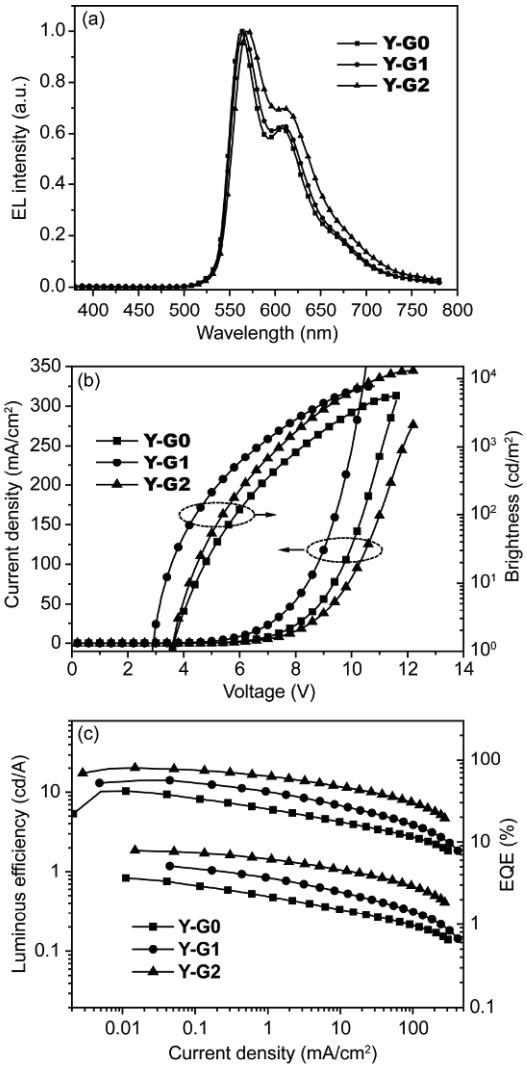

Figure 3 (a) EL spectra at the driving voltage of 8 V; the current density-voltage-brightness curves (b) and the luminous efficiency and EQE as a function of current density (c) of the non-doped devices.

that the excitons are mainly generated in the EML.

The current density-voltage-brightness curves, and the luminous efficiency and EQE as a function of current density are shown in Figure 3(b, c), respectively. And the related data are also tabulated in Table 2. All the dendrimers display a relatively low turn-on voltage (defined as the voltage at the brightness of 1 cd/m^2) of 3.0–3.6 V because of their high HOMO levels and the potential hole transport capability of carbazole dendrons. The maximum brightness is increased drastically from 5600 cd/m^2 of **Y-G0** to 13000 cd/m^2 of **Y-G2**, which may be reasonably ascribed to the reduced Ir-core interactions induced by the effective encapsulation from the outer dendrons. Among these dendrimers, **Y-G2** gives a luminous efficiency of 20.2 cd/A with EQE of 7.9%, about twice that of **Y-G0** (10.2 cd/A, 3.7%). In addition, **Y-G2** shows a slower efficiency roll-off compared with the other two dendrimers. At a brightness up to 1000 cd/m^2, the luminous efficiency of **Y-G2** remains at 12.1 cd/A, corresponding to an efficiency decrease of 40% relative to the maximum value. This value is much smaller than that of **Y-G0** (66%) and **Y-G1** (56%), which confirms that the exciton-exciton and exciton-polaron quenching could be inhibited by introducing carbazole dendrons into the periphery of Ir complex.

To further optimize the device efficiency, the doped device was fabricated by dispersing 10 wt% **Y-G2** into a host matrix *N*-(4-[9,3′;6′,9″]tercarbazol-9′-yl) phenylcarbazole (TCCz). In comparison to the corresponding non-doped devices, an enhanced performance is achieved, revealing a luminous efficiency of 32.1 cd/A, a power efficiency of 23.9 lm/W, an EQE of 11.6% together with a maximum brightness of 24500 cd/m^2 (Figure 4). The improvement indicates that the TCCz host can further reduce the intermolecular interactions in the film that cause exciton quenching.

Table 2 Device performance of the Ir dendrimers

Dopant	B (cd/m^2) [a]	η_L (cd/A) [b]	η_P (lm/W) [c]	EQE (%) [d]	λ_{max} (nm)	CIE (x, y)
Y-G0 (100 wt%)	5600	10.2	9.4	3.7	564	(0.51, 0.49)
Y-G1 (100 wt%)	7700	14.1	14.7	5.1	564	(0.52, 0.48)
Y-G2 (100 wt%)	13000	20.2	17.1	7.9	568	(0.53, 0.47)
Y-G2 (10 wt%)	24500	32.1	23.9	11.6	564	(0.52, 0.48)

a) Brightness; b) luminous efficiency; c) power efficiency; d) external quantum efficiency.

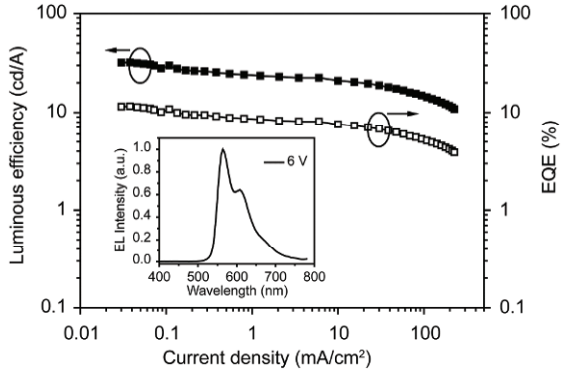

Figure 4 The luminous efficiency and EQE as a function of current density of the **Y-G2** based doped devices. Inset: EL spectrum of the device at 6 V.

4 Conclusions

In conclusion, we have reported the synthesis and characterization of a series of self-host yellow Ir dendrimers **Y-G0–Y-G2** containing carbazole dendrons. With the increasing generation number, the intermolecular interactions of the emissive Ir cores can be effectively prevented. Consequently, the luminous efficiency of the solution-processed non-doped OLEDs increases from 10.2 cd/A of **Y-G0** to 20.2 cd/A of **Y-G2**. By further dispersing the dendrimer **Y-G2** into a host matrix, the performance is improved to 32.1 cd/A. This work, we believe that, will shed light on the development of highly efficient yellow phosphorescent dendrimers with a self-host feature, and promote the realization of all-phosphor white OLEDs based on the dendrimer system.

Acknowledgments This work was supported by the National Natural Science Foundation of China (51573183, 21204084, 51203149, 51573182) and the National Basic Research Program of China (2015CB655000).

Conflict of interest The authors declare that they have no conflict of interest.

1 Yook KS, Lee JY. *Adv Mater*, 2014, 26: 4218–4233
2 So F, Krummacher B, Mathai MK, Poplavskyy D, Choulis SA, Choong VE. *J Appl Phys*, 2007, 102: 091101
3 Xiao LX, Chen ZJ, Qu B, Luo JX, Kong S, Gong QH, Kido JJ. *Adv Mater*, 2011, 23: 926–952
4 Aizawa N, Pu YJ, Watanabe M, Chiba T, Ideta K, Toyota N. *Nat Commun*, 2014, 5: 5756
5 Fan Q, Liu Y, Hao Z, Li C, Wang Y, Tan H, Zhu W, Cao Y. *Sci China Chem*, 2015, 58: 1152–1158
6 Wang D, Liu Q, Yu Y, Wu Y, Zhang X, Dong H, Ma L. *Sci China Chem*, 2015, 58: 993–998
7 Zhan X, Wu Z, Lin Y, Xie Y, Peng Q, Li Q, Ma D, Li Z. *Chem Sci* 2016, doi: 101039/c1036sc00559d
8 Lo SC, Burn PL. *Chem Rev*, 2007, 107: 1097–1116
9 Hwang SH, Moorefield CN, Newkome GR. *Chem Soc Rev*, 2008, 37: 2543–2557
10 Jung KM, Kim KH, Jin JI, Cho MJ, Choi DH. *J Polym Sci*, *Part A: Polym Chem*, 2008, 46: 7517–7533
11 Qin T, Ding J, Wang L, Baumgarten M, Zhou G, Muellen K. *J Am Chem Soc*, 2009, 131: 14329–14336
12 Ding J, Lu J, Cheng Y, Xie Z, Wang L, Jing X, Wang F. *Adv Funct Mater*, 2008, 18: 2754–2762
13 Ding J, Wang B, Yue Z, Yao B, Xie Z, Cheng Y, Wang L, Jing X, Wang F. *Angew Chem Int Ed*, 2009, 48: 6664–6666
14 Ding J, Zhang B, Lue J, Xie Z, Wang L, Jing X, Wang F. *Adv Mater*, 2009, 21: 4983–4986
15 Zhang B, Tan G, Lam CS, Yao B, Ho CL, Liu L, Xie Z, Wong WY, Ding J, Wang L. *Adv Mater*, 2012, 24: 1873–1877
16 Xia D, Wang B, Chen B, Wang S, Zhang B, Ding J, Wang L, Jing X, Wang F. *Angew Chem Int Ed*, 2014, 53: 1048–1052
17 Wang Y, Wang S, Zhao N, Gao B, Shao S, Ding J, Wang L, Jing X, Wang F. *Polym Chem*, 2015, 6: 1180–1191
18 Yu M, Wang S, Shao S, Ding J, Wang L, Jing X, Wang F. *J Mater Chem C*, 2015, 3: 861–869
19 Zhu M, Li Y, Hu S, Li Cg, Yang C, Wu H, Qin J, Cao Y. *Chem Commun*, 2012, 48: 2695–2697
20 Zhu M, Zou J, He X, Yang C, Wu H, Zhong C, Qin J, Cao Y. *Chem Mater*, 2012, 24: 174–180
21 Wu H, Zhou G, Zou J, Ho CL, Wong WY, Yang W, Peng J, Cao Y. *Adv Mater*, 2009, 21: 4181–4184
22 Zou J, Wu H, Lam CS, Wang C, Zhu J, Zhong C, Hu S, Ho CL, Zhou GJ, Wu H, Choy WCH, Peng J, Cao Y, Wong WY. *Adv Mater*, 2011, 23: 2976–2980